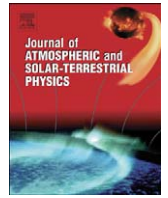




Contents lists available at ScienceDirect

Journal of Atmospheric and Solar-Terrestrial Physics

journal homepage: www.elsevier.com/locate/jastp

Plasmaspheric hiss overview and relation to chorus

Jacob Bortnik^{a,*}, Richard M. Thorne^a, Nigel P. Meredith^b^a Department of Atmospheric and Oceanic Sciences, University of California, Los Angeles, 405 Hilgard Avenue, Los Angeles, California 90095, USA^b British Antarctic Survey, Natural Environment Research Council, Madingley Road, Cambridge CB3 0ET, UK

ARTICLE INFO

Article history:

Accepted 25 March 2009

Available online 5 April 2009

Keywords:

Plasmaspheric hiss

Chorus

Very low frequency

Whistler waves

ABSTRACT

A brief overview is given of the history of plasmaspheric hiss research, particularly in the context of the recent work by Bortnik et al. (2008) indicating that chorus could be the likely source of plasmaspheric hiss. Previous suggestions given in the literature for this theory are reviewed and then the mechanism itself is outlined, focusing on the characteristic cyclical trajectories executed by typical ray paths that enter into the plasmasphere. A number of directional propagation studies performed in the past are then discussed as well as other work which bears relevance to the present mechanism.

© 2009 Elsevier Ltd. All rights reserved.

1. Introduction and background

Hiss was first discovered with the use of ground-based instruments, and described as a noise that ‘sounds like smooth hiss with a bandwidth of several kilocycles, and a center frequency of 3 or 4 kilocycles’ when played through a loudspeaker (e.g., Ellis, 1959). In one of the follow-up studies, Jorgensen (1966) observed that the hiss amplitude decreased with decreasing latitude, and concluded that the hiss emissions must have been generated in the auroral region and propagated down to lower latitudes. Follow-on studies confirmed this dependence of the hiss intensity upon latitude (Rao et al., 1972) but curiously, it was later shown that there was no direct correspondence between the mid-latitude and the auroral hiss spectra (Hayakawa et al., 1975). In the following years, studies performed with ground-based and low-altitude satellite data showed a variety of hiss morphologies, and different nomenclatures arose in an attempt to differentiate hiss according to its properties. For example, hiss was divided into ‘day time’ and ‘night time’ events (Harang, 1968), ‘steady-state’ and ‘disturbed’ hiss (Hayakawa et al., 1975), ‘morning side’ and ‘evening side’ events (Hayakawa et al., 1977), ‘narrowband 5 kHz hiss’ (Ondoh et al., 1980, 1981), ‘a steady hiss’ and a hiss with a latitude-dependent upper cutoff frequency (Ondoh et al., 1982, 1983), LHR and S-type hiss (Gross and Larocca, 1972), ELF hiss (Gurnett and O’Brien, 1964), ‘Band Limited Hiss’ (Muzzio and Angerami, 1972), ‘inner zone’ and ‘cutoff’ hiss (Smith et al., 1974), as well as the auroral and mid-latitude hiss signatures discussed above (Ellis, 1959) (to name but a few).

With the dawning of the high-altitude satellite era, a new type of hiss was identified, which had reasonably well-defined

properties: a wave observable with both electric and magnetic instruments (i.e., electromagnetic in nature) with an incoherent frequency–time structure, band limited to the typical frequency range ~200 Hz–2 kHz (though higher frequencies do occur at lower amplitudes), and generally confined to the high-density plasmasphere except for a zone of ‘apparent leakage’ at high latitudes predominantly in the afternoon sector (Russell et al., 1969; Muzzio and Angerami, 1972; Thorne et al., 1973, 1977, 1979; Kelley et al., 1975; Parady et al., 1975; and many more; see e.g., Hayakawa and Sazhin, 1992 for a review). This emission was called ‘plasmaspheric hiss’ due to its confinement within the plasmasphere and spectral resemblance to audible hiss. Plasmaspheric hiss was subsequently shown to be a critical component in governing the structure and dynamics of the Earth’s radiation belts. For example, hiss is specifically responsible for creating the slot region, which divides the region of trapped high-energy electrons into an inner and outer (radiation-belt) zone (e.g., Lyons et al., 1972; Lyons and Thorne, 1973; Meredith et al., 2007). More recently, it has been shown to be largely responsible for the quiet-time decay of outer radiation-belt electrons (Meredith et al., 2006a; Summers et al., 2007; Lam et al., 2007). Furthermore, plasmaspheric hiss is frequently observed in plumes (discuss further in Section 3.2) which might play an important role in radiation-belt dynamics (Summers et al., 2008). It is this particular emission which is the focus of the present discussion.

Early theories to explain the origin of hiss relied on the spontaneous growth of the background noise (i.e., the plasma emissivity) to observable levels due to the cyclotron instability (Thorne et al., 1973). This model conjectured that background-level waves near the outer edge of (but still within) the plasmasphere, and close to the geomagnetic equator would experience cyclotron growth due to unstable energetic electrons in the range ~10–50 keV, with sufficient anisotropy, and in fact would return to the equatorial region many times due to a ‘recycling’ process (Thorne et al., 1979). However, quantitative studies using ray

* Corresponding author. Tel.: +1 310 825 1659; fax: +1 310 206 5219.

E-mail addresses: jbortnik@atmos.ucla.edu (J. Bortnik), rmt@atmos.ucla.edu (R.M. Thorne), nmer@bas.ac.uk (N.P. Meredith).

tracing combined with path-integrated growth calculations, found that the overall amplitude gains were far too small to account for the observed hiss spectra, and the recycling process was not efficient enough to return a significant number of rays to the high-altitude amplification region (Huang and Goertz, 1983; Huang et al., 1983). This low gain was again found to occur in an extensive study, even when the most favorable conditions were assumed (Church and Thorne, 1983), which led the authors [*Ibid*] to suggest that the hot plasma could not amplify the incoherent background emissivity sufficiently, but some kind of weak 'embryonic source' of waves was needed for further amplification, which would require significantly less overall amplification to achieve observable levels. Three suggestions were listed towards the end of the paper, but not discussed or evaluated further. These suggestions for the embryonic source were:

1. Chorus emissions that enter the plasmasphere at high latitudes (i.e., the mechanism discussed in the present paper).
2. The low-frequency component of ducted whistlers that originate in lightning activity.
3. Propagation of auroral hiss or other auroral zone electromagnetic emissions into the plasmasphere near the ionospheric footprint of the plasmopause.

The mechanism of spontaneous cyclotron amplification of the background noise discussed above was referred to as '*in situ*' amplification of wave turbulence in later studies (e.g., Meredith et al., 2006b), because production of the waves occurred essentially where the wave itself appeared. In a few isolated cases, single transit amplification near the outer edge of the plasmasphere was indeed found to be sufficiently strong, but as we discuss further in Section 5, this is probably not representative of typical conditions, especially under disturbed geomagnetic conditions when plasmaspheric hiss intensity maximizes.

In addition to the *in situ* mechanism and the suggestion for embryonic sources, a large number of alternative mechanisms for the origin of hiss were examined. These mechanisms include:

1. An anthropogenic source of hiss, possibly due to power line harmonic radiation (PLHR) leaking into the plasmasphere from the ground (Parrot et al., 1991; Molchanov et al., 1991). In support of this mechanism, a modulation of mid-latitude hiss intensity by a ground-based VLF transmitter was reported, possibly related to its source (Dowden and Holzworth, 1990) (e.g., the "Sunday effect" when wave intensity would apparently be stronger during the work-week).
2. A 'long term' cyclotron instability mechanism with subsequent deformation of the particle distribution function (Etcheto et al., 1973; Bespalov and Trakhtengertz, 1986; Sazhin, 1984, 1989).
3. Hiss generation due to the proton cyclotron instability in the ring-current (Parady, 1974; Wang and Goldstein, 1988).
4. Hiss generation in the ionosphere due to unstable electron distributions, and subsequent propagation into the plasmasphere (Kovner et al., 1978).
5. Hiss generation in the ionosphere due to unstable proton distributions and subsequent outward propagation (Bud'ko, 1984).
6. A 'non linear' interaction mechanism (as opposed to linear or quasilinear, as employed in the '*in situ*' mechanism studied above), which could produce waves at highly oblique angles (Storey et al., 1991; Helliwell, 1989).
7. The evolution of lightning-generated ducted whistlers performing multiple hops between hemispheres and gradually degenerating into the hiss spectrum (Dowden, 1971).
8. The propagation and evolution of lightning-generated (non-

ducted) magnetospherically reflected whistlers into the incoherent hiss band, either as a trigger mechanism for spontaneous emission, as an embryonic source for further (modest) growth, or by themselves, without any further amplification (Sonwalkar and Inan, 1989; Draganov et al., 1992, 1993).

Of all the proposed mechanisms listed above, the lightning source (8) received the greatest attention and became the leading contender against the *in situ* mechanism.

As already mentioned, the *in situ* mechanism suffers from the fact that typical wave growth rates inside the plasmasphere are too modest to account for observed hiss intensities (Church and Thorne, 1983). However, if plasmaspheric hiss originated from lightning, the emissions would be expected to be stronger over the continents than over the oceans since lightning activity is more prevalent over land. A recent study of the geographic association of plasmaspheric emissions above 3 kHz (Green et al., 2005), led to substantial controversy (Thorne et al., 2006; Green et al., 2006). A more extensive study which resolved the various frequency-bands, showed that below 2 kHz, where the hiss emission power is strongest, there was no correlation between wave power and landmass (Meredith et al., 2006b), while the wave power >2 kHz had a high correlation with land. Whilst the lightning mechanism could explain many features of plasmaspheric hiss (Bortnik et al., 2003a, 2003b), it did not seem to be associated with the geographic distribution of lightning activity, and further could not directly account for the pronounced association of wave intensities with geomagnetic activity. There are several other issues concerning lightning as the origin of plasmaspheric hiss, but a discussion of these is deferred to Section 5. Clearly, an alternative explanation is required which is theoretically viable and can simultaneously account for all observed features of hiss.

The suggestion that hiss may be formed as a result of chorus that has propagated into the plasmasphere at high latitudes has received essentially no attention in the literature until the present study (Bortnik et al., 2008; Rodger and Clilverd, 2008), except for the single sentence quoted above from Church and Thorne (1983). However, hints of this association have recently begun to prevail in related studies, as discussed below.

2. Suggestions that chorus might be the source of plasmaspheric hiss

After a thorough ray-tracing-based study of the *in situ* generation of plasmaspheric hiss, Church and Thorne (1983) concluded that overall growth rates inside the plasmasphere were too small for spontaneous generation from the background incoherent emissivity levels. They made some tentative suggestions for what some of these embryonic sources could be, including that chorus might act as an embryonic source for further growth but not elaborating further on how this could function as a mechanism, or reproduce any of the observable properties of hiss. In the work by Bortnik et al. (2008), which we elaborate upon in the present paper, chorus is not regarded merely as an embryonic source for the further growth and generation of hiss, but it is shown that the plasmaspheric hiss resulting from the propagation of chorus into the plasmasphere occurs at power levels that are roughly comparable to the chorus itself. Of course, further modest amplification of the rays inside the plasmasphere is certainly possible and only strengthens the viability of this mechanism, resulting in longer lifetimes for the rays.

Another suggestion in the literature, linking chorus emissions with plasmaspheric hiss was made by Parrot et al. (2004). Using

wave data from the Cluster satellites, Parrot et al. (2003, 2004) observed isolated instances of chorus elements simultaneously propagating away from, and weak waves returning towards the geomagnetic equator. They interpreted this observation as a single group of chorus elements which propagated away from the equator, experienced a magnetospheric reflection (MR) at high latitudes, then returned to the equator at significantly reduced power levels. It was generally thought that under typical conditions, chorus only propagated away from its equatorial source region (e.g., LeDocq et al., 1998; Lauben et al., 2002), and did not return to the equator due to severe Landau damping that extinguished the ray before it could magnetospherically reflect (Bortnik et al., 2006). However, under conditions of lower flux levels, it was shown that such magnetospheric reflections could, in fact, occur [*ibid*] as observed. The observation of magnetospherically reflected chorus led Parrot et al. (2004) to speculate that the chorus could be a source of hiss and accumulate in a similar fashion to magnetospherically reflected whistlers generated by lightning (Draganov et al., 1992), though they caveat by saying that “the relation of hiss and chorus is, however, more complex and hiss bands have also been considered as sources of the chorus emissions (Koons, 1981)”. As shown in Section 3.3, the evolution of a single ray from chorus to hiss, depends not only on magnetospheric reflections as suggested by Parrot et al. (2004), but also on plasmopause reflections (PRs) interacting periodically with magnetospheric reflections to give cyclic ray trajectories within the plasmasphere, and thus dramatically longer ray lifetimes.

In a different set of studies, the propagation of unducted chorus elements from their source to the ground was studied by Chum and Santolik (2005) and a bifurcation of rays was observed (as in our studies) reflecting at low altitudes to either higher L or lower L depending on the initial wave normal angle of the ray at the equatorial source region of the chorus. It was shown that the rays reflecting to higher L were directly related to ELF hiss which is observed at higher latitudes and lower altitudes (Santolik et al., 2006), but a group of rays also reflected to lower L . This, together with previous experimental work (Santolik and Parrot, 1999), led Santolik et al. (2006) to speculate that the other group of rays reflecting to lower L (which were not examined further) could enter the plasmasphere and act as the embryonic source of hiss.

These recent suggestions are based on solid experimental evidence. However, until our recent study (Bortnik et al., 2008), they have not been examined further, and it was unclear how Landau damping or propagation effects might alter the entry of chorus into the plasmasphere if, in fact, Landau damping allowed the wave power to survive from its source, as far as the plasmasphere in the first place. It was also unclear how chorus could function as a mechanism, or reproduce any of the observable properties of hiss. The evolution of chorus into plasmaspheric hiss is discussed next.

3. Evolution of discrete chorus elements into plasmaspheric hiss

3.1. Mechanism overview

The entry of discrete chorus elements into the plasmasphere, and evolution into plasmaspheric hiss has been carefully modeled taking into account the L and magnetic local time (MLT) (day vs. night) dependence of cold-plasma density and suprathermal fluxes, an accurate model of latitude-dependent cold-plasma distribution, and a full distribution of wave normal angles (Bortnik et al., 2008). An illustration of the mechanism in a single, meridional plane is given in Fig. 1, where we schematically show the distribution of the wave frequency of hiss and chorus as

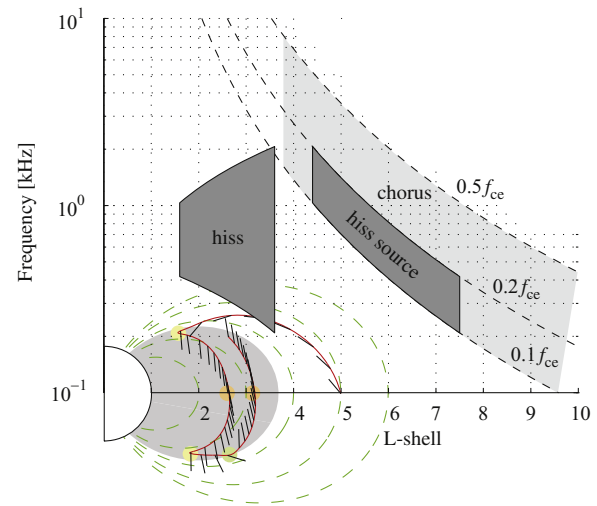


Fig. 1. Frequency spectrum of lower-band chorus (light-gray block, $L = 3.7$ – 10), and hiss (dark-gray block, $L = 1.5$ – 3.6), with the spectral region of waves that evolve from hiss into chorus marked as ‘hiss source’ (dark-gray block, $L = 4.5$ – 7.5). For reference, the Earth’s plasmasphere, and a single ray (c.f. Fig. 3) evolving from chorus into hiss are superimposed.

a function of L -shell. Lower-band chorus is typically found outside the plasmapause, as a series of short (~ 0.1 s), discrete, coherent elements, spanning the frequency range 0.1 – $0.5 f_{ce}$ (where f_{ce} is the equatorial gyrofrequency along that particular field line) (e.g., Burtis and Helliwell, 1976; Bortnik and Thorne, 2007). The typical frequency band as a function of L -shell is indicated in Fig. 1 as a light-gray region marked ‘chorus’.

Using careful ray tracing, Bortnik et al. (2008) showed that a certain subset of chorus propagates consistently from its source region in the plasmatrough, to the plasmasphere with minimal attenuation. This subset is indicated with a dark-gray region marked ‘hiss source’, and is characterized by low frequencies (~ 0.1 – $0.2 f_{ce}$) and medium wave normal angles (30 – 60°) directed towards the Earth. An example of a chorus ray that propagates into the plasmasphere is shown towards the bottom of Fig. 1, and a detailed discussion of this ray is given in Section 3.3.1. The inner edge of the ‘hiss source’ region is $\sim 1 L$ from the plasmapause, and all rays closer than the inner edge encounter the plasmapause at latitudes that are too low to establish cyclical trajectories (c.f. Section 3.3.1), where the wave normals experience large rotation to oblique angles and the chorus wave is rapidly Landau damped before entering the plasmasphere. In the present example, the plasmapause has been placed at $L \sim 3.6$ to simulate moderately disturbed conditions, and the inner edge of the hiss source region is located at $L = 4.5$. The outer edge of the hiss source region is defined by rays that are too far out to reach the plasmapause and become Landau damped before they are able to do so. Although isolated rays can still access the plasmasphere from higher L , the bulk of the chorus rays that enter the plasmasphere are located within $L \sim 7.5$, which is where we placed the outer boundary in Fig. 1 (see Fig. 2a of Bortnik et al. (2008)). Since the wave frequency of chorus decreases with increasing L -shell, the chorus rays propagating from the furthest regions of the hiss source also mark the lower-frequency cutoff of the hiss spectrum.

When the actual wave frequencies of the lower part of the chorus band (~ 0.1 – $0.2 f_{ce}$) are calculated over the hiss source region ($L \sim 4.5$ – 7.5), the frequency band of ~ 0.2 – 2 kHz is obtained, which corresponds precisely to the frequency band of hiss. While each chorus element starts off being coherent, each ray (initiated at a slightly different wave normal angle) crosses the plasmapause

at a slightly different location, and the wave loses its coherence almost immediately upon entering the plasmasphere, leading to the typical incoherent structure of hiss. Moreover, the frequency band of hiss tends to be slightly larger closer to the plasmapause than it is closer to the Earth (see e.g., Fig. 3 of Bortnik et al. (2008)), which is similar to the behavior obtained from ray tracing (not shown). Rays typically do not propagate inwards of $L \sim 1.5$, which is also similar to the observed distribution of hiss (Thorne et al., 1973).

Since chorus occurrence and intensity is highly dependant on geomagnetic conditions, and tends to occur predominantly during disturbed conditions (e.g., Meredith et al., 2001), it follows directly from our model that hiss occurrence and intensity should behave in a somewhat similar manner (disregarding propagation effects). In fact, it has been reported that hiss is indeed strongly dependant on geomagnetic activity, occurring predominantly in the aftermath of storms and during substorms (e.g., Smith et al., 1974; Meredith et al., 2004). According to our model, this may be related to the fact that the plasmapause needs to be at moderate L values for optimum access of chorus into the plasmasphere. If the plasmasphere becomes severely eroded, for instance during severe storms, access into the plasmasphere is more limited (and also shifts to higher frequencies) and the hiss intensities may not change much as had been observed (Smith et al., 1974). However, in the recovery phase of storms, the plasmasphere moves outwards due to refilling and access to the plasmasphere becomes favorable. This refilling, together with a high chorus occurrence rate, provides the optimal conditions for hiss formation, and is consistent with observations (Smith et al., 1974).

3.2. MLT distribution of chorus and hiss

Statistical studies show that the magnetic local time distribution of lower-band chorus is a function of magnetic latitude, with equatorial lower-band chorus peaking on the dawn-side, and mid-latitude lower-band chorus peaking on the day side (Meredith et al., 2001, 2003). This has recently been studied in greater detail and modeled by Bortnik et al. (2007a, 2007b), who again found that the MLT distribution varied dramatically as a function of the latitudinal range in which it was measured. For example, the low-frequency components of chorus ($0.1\text{--}0.2 f_{ce}$) had a distribution that peaked in the night and dawn sectors at low latitudes ($|\lambda| < 10^\circ$), but at high latitudes ($20^\circ < |\lambda| < 30^\circ$) had an intensity maximum in the afternoon sector. This was explained on the basis of Landau damping, which is essentially proportional to the number of ‘hot’ ($\sim 100\text{ eV}$ and above) electrons, divided by the number of ‘cold’ ($\sim 1\text{ eV}$) electrons, n_h/n_0 . This is illustrated in Fig. 2.

Fig. 2a shows a population of hot electrons convecting sunward from the plasmasheet, which drift east as they approach the Earth, and whose flux is lowered due to scattering by electrostatic electron cyclotron harmonic (ECH) waves and chorus (Horne et al., 2003; Bortnik et al., 2007a; Ni et al., 2008). Thus, the number of hot particles is high on the night side, and low on the day side. On the other hand, as illustrated in Fig. 2b, the Earth’s ionosphere is created by ionizing ultra-violet (UV) radiation from the sun (e.g., Kelley and Heelis, 1989), and thus is maximum on the day side and minimum on the night, leading to higher cold-plasma densities on the day side than on the night side (Carpenter and Anderson, 1992). The ratio n_h/n_0 is thus largest at night, leading to large damping and shorter propagation paths for chorus rays, and smallest on the dayside, leading to long propagation paths for chorus, a peak in the chorus power distribution at high latitudes (Bortnik et al., 2007a), and effective entry of chorus rays into the plasmasphere to evolve into hiss (Bortnik et al., 2008). As shown

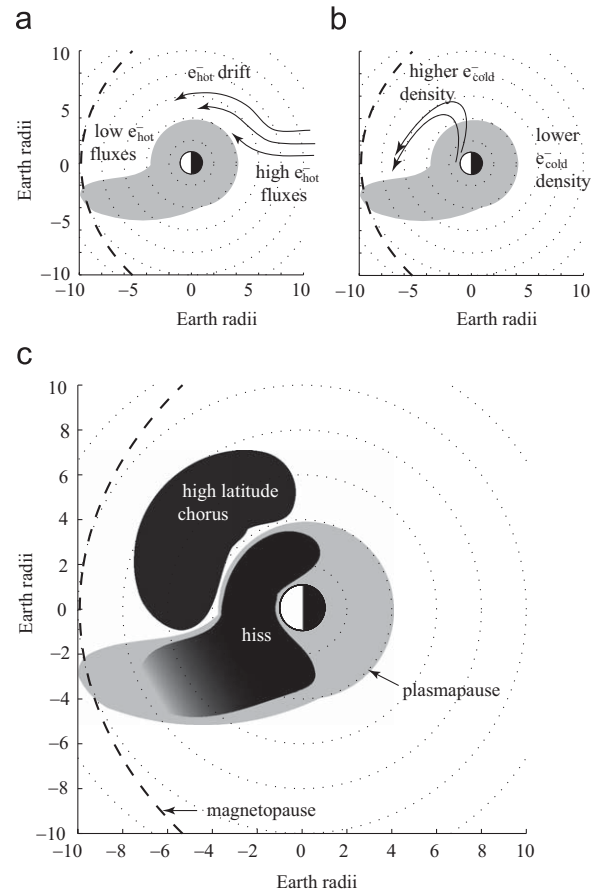


Fig. 2. MLT correspondence of hiss and chorus. (a) Hot plasmasheet electrons convecting sunward from the tail, forming a maximum on the night side, (b) cold ionospheric electrons flowing out to the magnetosphere, forming a maximum on the day side, and (c) MLT distribution of high-latitude chorus, and hiss, also indicating position of the plume.

schematically in Fig. 2c, the distribution of plasmaspheric hiss also tends to have a broad power maximum on the day side (Meredith et al., 2004) consistent with the high latitude entry of chorus. Since both chorus and plasmaspheric hiss intensify with increasing geomagnetic activity, there is a region in MLT where a plasmaspheric drainage plume forms (Goldstein et al., 2004) as shown in Fig. 2c, and thus there will not be direct MLT correlation between high-latitude chorus and hiss in this sector.

The ray tracing work shown in Section 3.3 and Bortnik et al. (2008) has been performed in a single meridional plane, i.e., it is a two-dimensional simulation with assumed symmetry in azimuth, which implicitly assumes that there are no strong gradients of the medium in MLT. This assumption is perfectly reasonable in the night and early afternoon sectors. However, in the later afternoon sector, the existence of a plasmaspheric drainage plume imposes a strong positive gradient of the electron number density with MLT ($\partial n_e / \partial \text{MLT} > 0$). Since chorus rays are generated at the source with a cone of wave normal angles, many of the rays will have wave vectors which have non-zero azimuth components. For example, a ray produced at the equator at $\text{MLT} = 1300$, oriented with $\psi = 30\text{--}60^\circ$ and $\phi = -90^\circ$ (pointing East) will propagate in azimuth (e.g., Muto and Hayakawa, 1987; Parrot et al., 2004) and will encounter the Western wall of the plasmaspheric drainage plume at high latitudes. The wave normal will then rotate towards the gradient of refractive index as expected from Snell’s law (i.e., the same effect that causes rays to propagate into the plasmasphere in Figs. 1, 3, and 4) and be pulled into the plume. The occurrence of hiss in plumes is a well-known and commonly

observed phenomenon (e.g., Summers et al., 2008), but chorus (in its typical coherent form) would necessarily be excluded from this region. Furthermore, since plumes often contain much embedded density structure, they are expected to have efficient guiding of rays to the ground in the late afternoon and evening sectors, but under normal conditions, hiss would generally remain confined within the plasmasphere and not be transmitted to the ground, as shown in Fig. 3.

3.3. Single ray example

Having described the large-scale features of the chorus–hiss mechanism, we now turn our attention to the details of the individual ray paths that evolve from chorus into hiss. As an example, we examine the ray injected with the following initial parameters: $L = 5$, day time (MLT = 15:00), geomagnetic equator ($\lambda_m = 0^\circ$), $0.1 f_{ce}$ (704 Hz), $\psi_0 = -40^\circ$. In Figs. 3 and 4, we show five separate panels indicating: (a) the ray path in geomagnetic coordinates, (b) the L -shell of the ray, (c) the latitude of the ray, (d) the unwrapped wave normal angle of the ray measured clockwise with respect to the negative B -field direction, and (e) the relative power of the ray, all as a function of group time. In calculating the relative power of the ray, we include the effects of Landau damping using realistic fluxes modeled from CRRES suprathermal electron data as described in Bortnik et al. (2007a), but in the present case we use an L -dependent distribution function, so that if a particular ray happens to cross L -shells, the correct distribution function is automatically selected in the calculation. The relative power also includes the effects of magnetic field-line convergence, so that if a ray propagates closer to the Earth, its wave power increases in inverse proportion to the azimuthal arclength variation (see Bortnik et al. (2007b) for a formula). The colored circles in panel (a) correspond to key propagation features as described in the figure caption.

3.3.1. Ray example: first 5 s

Fig. 3 illustrates the first 5 s of the wave propagation. In panel (a) we show the ray path in red with attached short, black line-segments at regular intervals that represent the wave normal angle. Detailed propagation features are as follows.

At $t = 0$ s, the ray is injected at the equator, and propagates to higher latitudes. Initially, the ray experiences Landau damping due to its oblique angle ($\psi_0 = -40^\circ$ measured clockwise relative to the $+B$ -field direction or $\psi_0 = +140^\circ$ measured clockwise relative to the $-B$ -field direction), and a decrease in relative power ensues (panel (e)). As the ray propagates further, the wave normal angle progressively rotates in a clockwise direction due to the natural density and B -field gradients, such that at mid-latitudes ($\sim 15^\circ$ – 35° near $t \sim 0.3$ s, panel (c)), the wave normal angle is roughly field aligned (panel (d)) and Landau damping becomes ineffective since the E_z component of the wave tends to zero. Simultaneously, the ray propagates to higher latitudes and lower altitudes such that its relative power increases due to the field-line convergence, and power increases ~ 1.5 times above its original value. At this high latitude part of its trajectory ($t \sim 0.8$ s), the wave normal angle rotates down from $\psi \sim 180^\circ$ through $\psi = 90^\circ$, and reverses its direction of travel in a so-called magnetospheric reflection. This MR is further aided by the fact that at this high latitude, the ray is grazing the plasmapause and the large inward gradient in plasma density tends to rotate the wave normal such that it is perpendicular to the plasmapause (analogously with the well-known Snell's law from geometrical optics). This entry into the plasmasphere through the MR mechanism is indicated in panel (a) with the yellow circle, and with the yellow bar in panels (b)–(e).

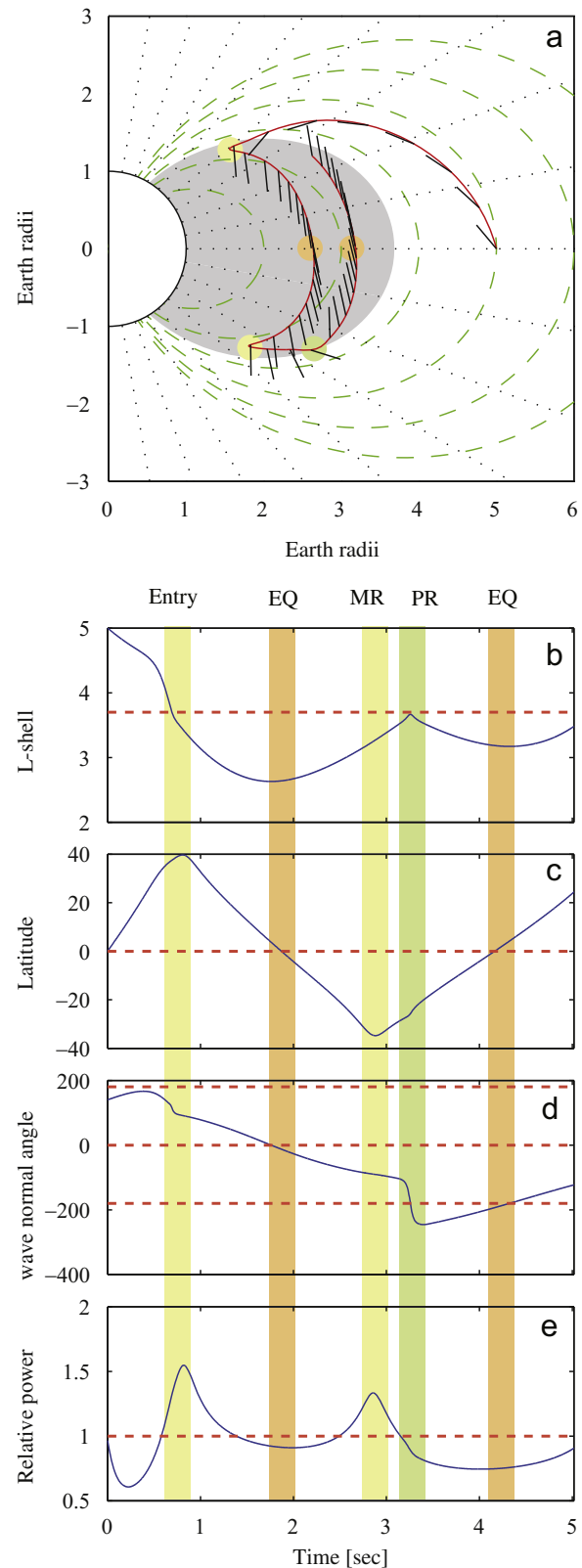


Fig. 3. The first 5 s of propagation of the ray described in Section 3.3.1. (a) Ray path, (b) L -shell, (c) latitude, (d) wave normal angle measured counterclockwise from the $-B$ direction, and (e) relative power of the ray. The colored circles in panel (a) correspond to magnetospheric reflection (yellow), equatorial crossing (brown) and plasmapause reflection (green), and correspond to the similarly colored bars in the right-hand panels. (For interpretation of the references to color in this figure legend, the reader is referred to the web version of this article.)

After entering the plasmasphere at high latitudes, the ray propagates to low latitudes at low L -shells, and crosses the geomagnetic equator at $L \sim 2.6$. This first equatorial crossing (EQ) is marked in panel (a) with a brown circle, and a corresponding brown bar in panels (b)–(e). Due to the geometry of the ray entry, its wave normal angle is oriented in such a way that it is essentially field aligned during the first equatorial crossing ($t \sim 1.9$ s, panel (d)). We also note at this point that the relative wave power of the ray is $> 90\%$ of its original value (panel (e)), due to the fact that magnetic field-line convergence has compensated for the initial Landau damping experienced by the ray.

After the first equatorial crossing, the wave normal continues to rotate due to the natural plasma density and B -field gradients, until the wave normal angle becomes sufficiently oblique that the ray experiences another MR at $t \sim 2.9$ s. The ray propagates to higher L and encounters the plasmopause at $t \sim 3.25$ s. At this point, the large negative density gradient causes the wave normal angle to rapidly rotate towards lower L -shells, the ray path consequently rapidly changes direction and begins propagating to lower L , and the ray essentially experiences a plasmopause reflection. This PR is indicated in panel (a) with a green circle, and with a green bar in panels (b)–(e). The dashed line in panel (b) gives the approximate location of the plasmopause, so that the behavior of the PR becomes more obvious. The rapid change of wave normal angle is shown in panel (d). Since the natural tendency is for the wave normal to rotate towards higher L , as the ray continues along its propagation path, the wave normal again crosses the geomagnetic equator with an almost field-aligned wave normal (panel (d)), as highlighted by the second brown bar at $t \sim 4.25$ s.

Since the ray is field-aligned when it crosses the equator in the first few seconds of propagation, it could experience further modest amplification which would extend its lifetime beyond our present calculations (which assume no wave growth). In addition, if there are any density enhancements present (i.e., ducts) the wave normal would naturally fall within the trapping cone and be transmitted (guided) to the ground. In the absence of such structure, the ray will only be observable in the plasmasphere.

We have thus described the essential elements of the ray propagation: MR at high latitudes and entry into the plasmasphere, field-aligned equatorial crossings, and MR followed by PR, which lead to further (roughly) field-aligned equatorial crossings. Next, we examine the entire lifetime of the ray.

3.3.2. Ray example: full lifetime

Fig. 4 shows the ray described above, but for the entire 17.8 s lifetime, with colored circles and bars as described above. From panel (a), the ray path is seen to undergo a ‘cyclic’ trajectory inside the plasmasphere, which consists of a pattern moving between low and high L -shells. This is illustrated in panels (b)–(d), where the ray undergoes a well-defined sequence of reflections and equatorial crossings in the order: (MR–EQ–MR)–(PR–EQ–PR)–(MR–EQ–MR)–, etc. Panel (d) shows that whenever the ray crosses the equator, its wave normal angle is roughly field-aligned (an integer multiple of 180°), in agreement with recent observations that have indicated that plasmaspheric hiss occurs with roughly field-aligned wave normal angles (Santolik et al., 2001).

Since Landau damping is most efficient for waves with large wave normal angles near the equatorial plane, the fact that our rays cross the equator with essentially field-aligned wave normal angles means that there is very little overall Landau damping that affects the ray, allowing it to survive unattenuated for an extended period of time. This is seen in panel (e), where the variations in relative wave power are controlled primarily by the position of the ray, becoming more intense closer to the Earth due to magnetic

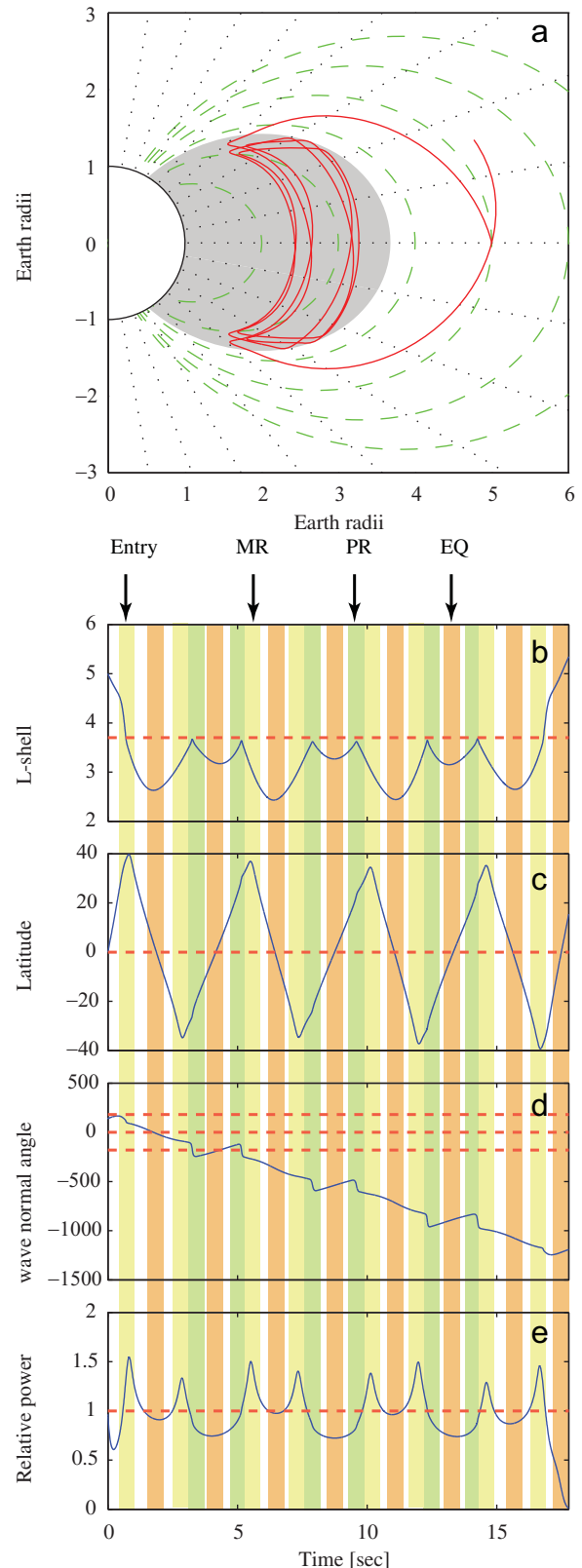


Fig. 4. The full lifetime of the ray shown in Fig. 3, with corresponding panels and color designations.

field-line convergence, and conversely, less intense further way from the Earth. There is little overall loss of power due to damping on timescales of tens of seconds.

Since the ray trajectory is not precisely cyclic, but has small fluctuations, the wave normal angle impinges on the plasmapause every time with small, random fluctuations. Eventually at $t \sim 17$ s, the wave normal becomes sufficiently perpendicular to the plasmapause that the ray does not undergo a PR, but is able to escape from the plasmasphere, and travel back out to higher L -shells. In so doing, the wave normal becomes more oblique, and the damping rate increases due to the low cold-plasma density and high suprathermal fluxes, resulting in rapid Landau damping of the ray. As shown, the ray is only able to cross the magnetic equator once, and is completely damped thereafter.

Fig. 4 illustrates that rays that enter, and become trapped within the plasmasphere can remain trapped for many tens of seconds with minor losses due to Landau damping. If it were not for the de-trapping of the ray, it could have continued its cyclic trajectory inside the plasmasphere, as many of the chorus rays do. Some of the rays reach lifetimes in excess of 100 s. A similar process which causes de-trapping of the rays (i.e., minor random fluctuations in the PR process) can also break the cyclic trajectory shown in Fig. 4a, and cause the ray to remain trapped within the plasmasphere and only magnetospherically reflect between the northern and southern hemisphere without PR. Since this MR process causes the rays to have equatorial crossings with large wave normal angles, the wave power proceeds to decay due to Landau damping. In the process, however, such rays would form a second population of rays that have large, outward-pointing wave normal angles.

It is interesting to note that the cyclic trajectory of the ray, results in two separate zones of enhanced hiss wave power near the equatorial plane. In the case shown in Fig. 4, the division of the zones is at $L \sim 2.5$, but the exact location of this division is a function of the wave frequency, and the entry latitude of the chorus ray into the plasmasphere. This entry latitude is, in turn, a function of the equatorial source region of the chorus ray itself, with chorus rays originating at higher L , entering the plasmasphere at higher latitudes (and vice versa). In general, the division into two zones falls in the region $L \sim 2$ – 2.5 . In addition, hiss in the inner zone should exhibit greater amplitude variability since it contains the first hop of the wave after its entry into the plasmasphere (which should be roughly correlated to the original chorus element). These theoretical consequences of our model have been reported by Tsurutani et al. (1975), who have reported a division of hiss into an inner and outer zone, separated roughly at $L \sim 2$, with the inner zone exhibiting greater variability and the outer zone being relatively smoother and more stable.

The above example ray has shown a single, representative ray that enters the plasmasphere and undergoes a cyclic trajectory tens of seconds. This cyclic trajectory causes the ray to traverse the magnetic equatorial plane with roughly field-aligned wave normal angles, such that Landau damping is ineffective and the wave power remains at levels that are comparable to its original wave power in the chorus source region. Due to the effects of field-line convergence, the wave power can sometimes even exceed its original value (in our example by up to $\sim 50\%$). The rays (which have evolved into plasmaspheric hiss) are removed from the plasmasphere by either becoming de-trapped and leaking back out through the plasmapause, or attaining high wave normal angles within the plasmasphere and becoming Landau damped. In either case, chorus waves that were present outside the plasmasphere for tenths of a second, can propagate into the plasmasphere and remain trapped for tens of seconds, such that the repeated injection of chorus wave power from individual chorus elements, causes a build-up of incoherent wave power inside the plasmasphere, in the critical frequency range ~ 0.2 – 2 kHz, forming plasmaspheric hiss.

4. Relation to previous directional studies

Since our hiss generation mechanism relies on a number of assumptions, and makes specific predictions regarding wave normal and propagation directions of both chorus and hiss, it is instructive to examine these assumptions and predictions in the light of past studies.

In the present study, we have assumed that rays are produced in the chorus source region with all allowable wave normal angles, from $-\psi_{\text{res}}$ to $+\psi_{\text{res}}$ (where ψ_{res} is the resonance cone angle, beyond which propagation is not allowed in cold plasma). There are two important caveats to note: first, it is certainly true, and can be expected on theoretical grounds that a ‘small’ radiating structure embedded within a plasma will radiate waves over a broad range of wave normal angles (e.g., Stenzel, 1976). This is true for antennas whose scale is small compared to the wavelength of the wave (Balmain, 1964; Fisher and Gould, 1969; Wang and Bell, 1969, 1972, 1973), and is equally true for natural radiating structures spontaneously formed within the plasma, such as a group of non-gyrotropic, phase-bunched electrons which can be thought of as a helical antenna (Helliwell and Crystal, 1973; Helliwell and Inan, 1982; Carlson et al., 1990). To support the latter claim, estimates of the dimension of the chorus source region perpendicular to the magnetic field are on the order of 10 km, which is on the order of a wavelength, or even less (Santolik and Gurnett, 2003; Santolik et al., 2004). On the other hand, to produce a true plane wave, the source either needs to be infinitely large, or be located infinitely far away from the observer, so we can safely conclude that there will be more than a single plane wave present in the source region. The second important caveat is that the radiated wave power is not, in general, expected to be uniform in all directions, but instead will have some specific radiation pattern (i.e., distribution of wave power as a function of wave normal angle) dependant on the geometry of the radiating structure, and its orientation in the plasma. The task then becomes to place some constraints on the radiation pattern of chorus in its source region.

There have been several studies of chorus wave normal angles in the past, the majority of which show that near the chorus source region, wave normal angles are generally clustered around the magnetic field direction within a cone of half-angle ~ 10 – 20° (Burton and Holzer, 1974; Goldstein and Tsurutani, 1984; Hayakawa et al., 1984; Santolik et al., 2003). However, in all of the above studies, even though the majority of wave normal measurements showed small angles, there was inevitably a certain number of cases showing very large wave normals, possibly indicating that the majority of the chorus wave power was emitted in a field-aligned direction with decreasing power emitted at increasing wave normal angles. Using backward ray tracing from off-equatorial locations of measured chorus wave normals, a number of authors have shown that the only way to record the given wave characteristics at the observed location would be to generate that particular group of rays at highly oblique angles (Lauben et al., 2002; Parrot et al., 2004; Inan et al., 2004; Santolik et al., 2006; Brenemann et al., 2007). The global distribution of chorus intensity has recently been shown to be most consistent with chorus waves that are generated in a field-aligned direction (Bortnik et al., 2007a), but again, the access of chorus to low altitudes with significant power indicates that there is also a (possibly weaker) component of chorus present at high wave normals (Santolik et al., 2006; Bortnik et al., 2007b).

In the analysis of Bortnik et al. (2008), which is discussed further herein, we have chosen to treat the most general case, and inject rays with all allowable wave normal angles from $-\psi_{\text{res}}$ to $+\psi_{\text{res}}$ but we have not specified how power is distributed over that range of angles. There are three possible scenarios illustrated in

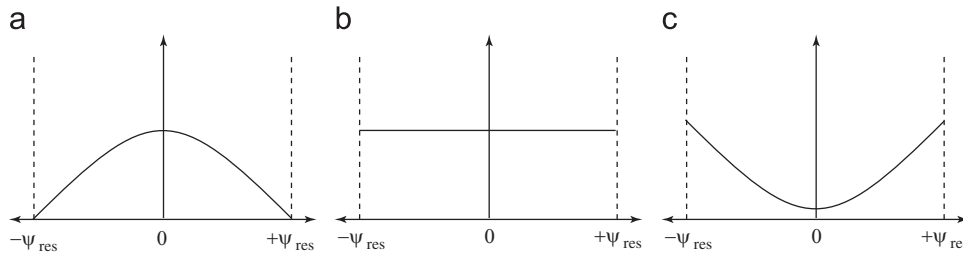


Fig. 5. Schematic representation of three possible distributions of wave power as a function of wave normal angle (radiation pattern), of chorus. (a) Peaked in a field-aligned direction, decreasing to high wave normal angles, (b) isotropic, and (c) peaked at high wave normal angles.

Fig. 5: (a) wave power is peaked in a field-aligned direction and decreases with increasing wave normal angle (which we believe is the most likely), (b) a roughly isotropic distribution of wave power with wave normal angle, and (c) a distribution which minimizes in a field-aligned direction, and peaks at high wave normal angles. Whatever the case, from our analysis, the key range of wave normal angles that evolve into hiss is roughly $\psi_0 \sim -30^\circ$ to -60° which is sufficiently intermediate between low and high wave normal angles that it should be present regardless of the radiation pattern assumed. Wave normals in this range have been directly measured at the source, and inferred from remote measurements as described above, making our assumptions of a source with broad wave normal distribution very reasonable.

Once the chorus waves enter the plasmasphere at high latitudes and begin to propagate within the plasmasphere, they enter a period where they undergo ‘cyclic’ trajectories as shown above, until they either escape from the plasmasphere again, or become oblique and are Landau damped. Thus, we expect that within the plasmasphere, a large portion of the hiss wave power will be field-aligned near the equator, with some smaller portion of the wave power at higher wave normal angles. Past studies of hiss wave normal angle distributions have generally shown mixed results, indicating either highly oblique wave normal angles (Storey et al., 1991), a broad spectrum of wave normal angles extending from $\psi \sim 0^\circ$ to $\psi \sim \psi_{res}$ (Parrot and Lefeuvre, 1986), or groupings, e.g., Hayakawa et al. (1986) who found field-aligned wave with $\psi \sim 0^\circ$, or others with large wave normal angles of $\psi \sim 70\text{--}80^\circ$. The analysis of hiss wave normal distributions is complicated by the fact that hiss is an incoherent emission, often having multiple waves present simultaneously which violates the ‘plane wave’ assumption inherent in most direction finding algorithms. However, in a recent study, Santolik et al. (2001) used the wave distribution function analysis technique (which accounts for multiple wave present simultaneously) (Storey and Lefeuvre, 1979) on a short segment of POLAR PWI data to show that there is strong clustering of wave normal angles (ψ) around the ambient field direction, at $\psi \sim 0^\circ$ and 180° at $L \sim 3.5\text{--}3.7$. This recent analysis is consistent with our expectation that there will be a strong grouping of hiss wave power at small wave normal angles. As mentioned above, from single ray examples, we expect that the mixed observational results discussed above will be consistent with the rays that have broken out of their cyclic trajectories and become oblique within the plasmasphere, and appear together with the field-aligned wave population.

5. Relation to selected emission mechanisms

As discussed in Section 1, ray tracing combined with growth calculations using an average statistical distribution of cold and hot electrons showed that, generally, the overall gain was significantly too small to produce hiss *in situ* within the plasma-

sphere (Church and Thorne, 1983; Huang and Goertz, 1983; Huang et al., 1983). However, in two studies using measured wave and particle distributions, it was indeed found that single-pass growth rates were sufficiently large to allow observable intensities of hiss to be generated from the background noise (Cornilleau-Wehrlin et al., 1985; Solomon et al., 1988), raising the question whether *in situ* growth could account for the hiss spectrum after all. We believe that even though the above studies did show high gain, they were probably not representative of typical hiss characteristics. The observations were taken at relatively high L -shells ($L \sim 4.5\text{--}5.2$), where growth rates are naturally much higher than at lower L -shells. Typically, the most intense hiss is observed at $L \sim 3$, and its intensity increases with increasing geomagnetic activity (e.g., Meredith et al., 2004). When geomagnetic activity increases, the plasmapause erodes and moves to lower L -shells, typically $L \sim 3\text{--}4$, where growth rates become negligible due to increased electron resonant energy (> 100 keV). In the above studies, the plasmapause was located well beyond $L = 5$ (and sometimes even beyond $L = 5.5$), indicating very quiet conditions which are not typical of the most intense hiss. Moreover, the higher-energy electrons necessary for growth at lower L -shells tend to drift further out in L -shell than the lower energy electrons, so the flux of particles available for cyclotron growth at lower L -shells would be further reduced. Even if the source of quiet-time hiss was in the outer plasmasphere as suggested by the above studies, it could still not account for the hiss observed at much lower L -shells ($L \sim 1.5$), and would presumably require waves to propagate inwards, similar to previous ray tracing studies (Church and Thorne, 1983; Huang and Goertz, 1983; Huang et al., 1983). If that were true, than those rays which are on cyclic trajectories would traverse the source region multiple times and would grow to enormous intensities in the matter of several seconds, which is inconsistent with observations. Thus, we believe that the work of Solomon et al. (1988) and Cornilleau-Wehrlin et al. (1985) may not be representative of intense hiss under typical conditions.

A second point of discussion is that hiss (or exo-hiss) has been previously invoked as the trigger mechanism that generates chorus (e.g., Koons, 1981). This idea was proposed due to the frequent observation of chorus occurring simultaneously with a hiss band, and often with chorus seeming to rise out of the upper cutoff frequency of the hiss (Burtis and Helliwell, 1969, 1976; Cornilleau-Wehrlin et al., 1978; Koons, 1981; Hattori et al., 1991). The idea that hiss-triggered chorus emissions was subsequently used in a number of theories describing the chorus source mechanism (e.g., Trakhtengerts, 1999; Nunn and Sazhin, 1991; see Omura et al., 1991 for review). However, we believe that our mechanism explains the often simultaneous occurrence of hiss and chorus—simply due to the fact that chorus propagates into the plasmasphere, degenerates into the hiss band, which then leaks back out into the plasmatrough (see Figs. 1 and 3 of Bortnik et al. (2008)) and appears together with the chorus. Since this process only takes a few seconds, it is almost impossible to

distinguish which wave came first. There are many specific instances of chorus observations in the data (particularly on the night side) where hiss is not simultaneously visible, which calls into question the idea that chorus is always triggered from the top of the hiss band (e.g., Hattori et al., 1991, p. 1466, point (3)). The most recent (and most advanced) theoretical models of chorus generation do not rely on hiss triggering, and have produced realistic chorus elements directly from the background noise levels (Katoh and Omura, 2007; Omura et al., 2008).

Finally, we make mention of the lightning source of hiss (Sonwalkar and Inan, 1989). In this theory, terrestrial cloud-to-ground lightning discharges radiate electromagnetic energy through the ionosphere and into the non-ducted mode of propagation into space (Draganov et al., 1992, 1993). At the point of injection of the rays into space, the spectral intensity maximizes at $\sim 4\text{--}5$ kHz, but as the rays propagate the higher frequency components become preferentially Landau damped, and only the lower-frequency wave components survive for appreciable periods, accounting for the frequency band at < 1 kHz (Bortnik et al., 2003a, 2003b).

While this theory for the origin of hiss is by all means plausible, and in our opinion still contributes some wave power into the hiss band, it does not reproduce all the observed hiss features. There are a few noteworthy examples:

- a. *Wave normal*: While lightning-generated MR whistler evolution into hiss gives qualitatively good agreement with the hiss bandwidth, the wave normal angles of hiss are observed to be predominantly field-aligned (e.g., Fig. 1 of Santolik et al., 2001), whereas the MR mechanism would necessarily give highly oblique waves. On the other hand, the chorus mechanism produces approximately field-aligned hiss waves on every equatorial traverse of the waves as shown above. In some instances, an additional population of high wave normals is observed in addition to the field-aligned population, which might have originated from lightning, but it may also have originated from evolved chorus rays that have broken out of their cyclical plasmaspheric trajectories.
- b. *Frequency distribution with L* : According to the MR whistler mechanism, each frequency component of the lightning spectrum would tend to settle on an L -shell where the lower hybrid resonance frequency matches the wave frequency. This behavior results in a distribution with a rising frequency towards lower L -shells, which is not the observed distribution of hiss. In fact, CRRES data do show such a wave component, following the LHR, but it is significantly lower in power than the traditional hiss band, about two orders of magnitude lower or more, and numerical simulations reproduce this lightning-generated wave band (Chum and Santolik, 2005). We note in passing, that this band is not the same as the intense wave band observed at or below the LHR frequency, which is composed of magnetosonic waves, is restricted $\pm 3^\circ$ about the geomagnetic equator, and has its source in the unstable proton population (Meredith et al., 2008).
- c. The hiss wave power below 1 kHz is not correlated with land masses, which would be expected if lightning were its main source (Meredith et al., 2006b) since lightning is mostly confined to land. However, the wave power > 2 kHz is indeed well correlated with landmasses (Green et al., 2005; Meredith et al., 2006b). On the other hand, the hiss wave component < 1 kHz is well correlated with geomagnetic activity, which is not consistent with the lightning mechanism since lightning flash rates are clearly independent of geomagnetic activity. We do note, however, that it may still be possible to achieve some degree of geomagnetic control indirectly for the lightning
- d. Another reason why lightning may not be the source of hiss, is the discrepancy in MLT distributions of the low- and high-frequency components. The low-amplitude, high-frequency (2–5 kHz) portion of the frequency spectrum has a maximum amplitude in the 18–24 MLT sector (Fig. 8, Meredith et al., 2006b) as expected for the lightning-generated source, due to its high lightning prevalence and lower D-region attenuation. In contrast, the high-amplitude, low-frequency (0.1–2 kHz) portion of the spectrum, which is the typical frequency band of plasmaspheric hiss, has a maximum amplitude in the 6–12 MLT sector, which is a region of weak lightning activity and strong D-region attenuation. This suggests that the low-frequency waves in the pre-noon sector are not generated by lightning.
- e. The most convincing argument (to this author) though, is the behavior of the hiss frequency bandwidth as a function of L . Since higher frequency components become Landau damped more rapidly than lower-frequency components, we would expect to find a larger bandwidth (containing more power in high-frequency components) closer to the source, and becoming smaller in the direction away from the source. With lightning, the bandwidth would be largest in low to middle L -shells ($L \sim 1.5\text{--}2$), and decreasing with increasing L towards the plasmapause. However, the data shows the opposite behavior. The largest bandwidth of hiss is seen near the plasmapause, and decreases as L becomes lower. This is seen in Fig. 3 of Bortnik et al. (2008), as well as in statistical distributions (Thorne et al., 1973). On the other hand, the resulting bandwidth from our ray tracing simulations reproduce this behavior precisely.

6. Summary

In this paper, we gave a brief historic overview of a few selected mechanisms that were proposed as the origin of plasmaspheric hiss. We pointed out that there were a significant number of mechanisms in the past literature that were carefully examined, and then focused on the few specific suggestions of chorus as the origin of hiss, that were not examined in detail but nevertheless form the backdrop for the present mechanism.

We then provided a brief schematic overview of the mechanism that causes whistler-mode chorus in the ELF/VLF frequency band to evolve into plasmaspheric hiss, its dependence on L -shell, and frequency band. Our model naturally accounts for the essential features of hiss, such as the observed frequency spectrum, its incoherent nature, the day–night asymmetry in intensity, the distribution in L , and the geomagnetic control as well as other ancillary features, such as the two-zone structure of hiss, exo-hiss and ELF hiss.

The MLT asymmetry in hiss was related to the propagation characteristics of chorus, namely the lowered levels of Landau damping of chorus on the day side relative to the night side, which causes a longer path length of chorus on the day side. There is also a region of MLT in the post-noon sector where hiss is observed but chorus is not, believed to be related to the formation of a plasmaspheric drainage plume. This plume necessarily excludes chorus, but frequently contains hiss, believed to have leaked in from the plasmatrough similarly to the high-latitude entry mechanism we have shown above. A ray trajectory of a single, typical ray that evolves from chorus into hiss was examined, and it was shown that such rays can occur at essentially the same power

levels as the original chorus rays, perform cyclical trajectories within the plasmasphere, and cross the equator at roughly field-aligned wave normal angles.

We then discussed our mechanism in light of past studies that analyzed both chorus and hiss in terms of their directionality, i.e., direction of propagation and wave normal angle distribution. We showed that the most likely scenario is that chorus is generated with a broad distribution of wave normal angles in the source region, which is probably peaked in power in the field-aligned direction, but nevertheless contains significant power at high wave normals. This broad wave normal distribution is precisely what we have modeled in the present work, and have shown that a variety of possible behaviors are obtained in different wave normal regions within the distribution, including the evolution of chorus into plasmaspheric hiss. Finally, we discussed a few selected generation mechanisms of both hiss and chorus, and have briefly commented on why we believe that the lightning mechanism may not be able to account for all the observed characteristics that constitute the source of plasmaspheric hiss.

Acknowledgements

J.B. would like to acknowledge support from the National Science Foundation's (NSF) Geospace Environment Modeling (GEM) post-doctoral award ATM 0621724, and J.B. and R.M.T. would like to acknowledge support from NASA grant NNX08A135G. NPM would like to acknowledge support from the Natural Environment Research Council, UK. The authors thank Roger R. Anderson for provision of the CRRES plasma wave data used in this study. This manuscript is based on material which was originally presented as the Supplementary Information of Bortnik et al. (2008), and has been extensively modified and extended for the present Special Issue on the Inner Magnetosphere.

References

- Balmain, K.G., 1964. The impedance of a short dipole antenna in a magnetoplasma. *IEEE Trans. Antennas Propagation* 12 (5), 605–617.
- Brenemann, A., Kletzing, C.A., Chum, J., Santolik, O., Gurnett, D., Pickett, J., 2007. Multispacecraft observations of chorus dispersion and source location. *J. Geophys. Res.* 112 (A5), A05221.
- Bespalov, P. A., Trakhtengertz, V. Yu., 1986. Cyclotron instability of the Earth's radiation belts. In: Leontovich, M. A. (Ed.), *Reviews of Plasma Physics*, (English translation). Vol. 10. pp. 155–292.
- Bortnik, J., Inan, U.S., Bell, T.F., 2003a. Frequency-time spectra of magnetospherically reflecting whistlers in the plasmasphere. *J. Geophys. Res.* 108 (A1).
- Bortnik, J., Inan, U.S., Bell, T.F., 2003b. Energy distribution and lifetime of magnetospherically reflecting whistlers in the plasmasphere. *J. Geophys. Res.* 108 (A5).
- Bortnik, J., Inan, U.S., Bell, T.F., 2006. Landau damping and resultant unidirectional propagation of chorus waves. *Geophys. Res. Lett.* 33, L03102.
- Bortnik, J., Thorne, R.M., Meredith, N.P., 2007a. Modeling the propagation characteristics of chorus using CRRES suprathermal electron fluxes. *J. Geophys. Res.* 112, A08204.
- Bortnik, J., Thorne, R.M., Meredith, N.P., Santolik, O., 2007b. Ray tracing of penetrating chorus and its implications for the radiation belts. *Geophys. Res. Lett.* 34 (15), L15109.
- Bortnik, J., Thorne, R.M., 2007. The dual role of ELF/VLF chorus waves in the acceleration and precipitation of radiation belt electrons. *J. Atmos. Sol. Terr. Phys.*, Special Issue: Global Aspects of Magnetosphere-Ionosphere Coupling 67, 378–386.
- Bortnik, J., Thorne, R.M., Meredith, N.P., 2008. The unexpected origin of plasmaspheric hiss from discrete chorus emissions. *Nature* 452 (7183), 62–66.
- Bud'ko, N.I., 1984. Generation of ELF hiss in the ionosphere by proton fluxes. *Geomagn. Aeron.*, (English translation) 24, 291.
- Burtis, W.J., Helliwell, R.A., 1969. Banded chorus—a new type of VLF radiation observed in the Magnetosphere by OGO 1 and OGO 3. *J. Geophys. Res.* 74 (11), 3002–3010.
- Burtis, W.J., Helliwell, R.A., 1976. Magnetospheric chorus: occurrence patterns and normalized frequency. *Planet. Space Sci.* 24 (11), 1007.
- Burton, R.K., Holzer, R.E., 1974. The origin and propagation of chorus in the outer magnetosphere. *J. Geophys. Res.* 79, 1014–1023.
- Carlson, C.R., Helliwell, R.A., Inan, U.S., 1990. Space-time evolution of whistler mode wave growth in the magnetosphere. *J. Geophys. Res.* 95, 15073.
- Carpenter, D.L., Anderson, R.R., 1992. An ISEE/whistler model of equatorial electron density in the magnetosphere. *J. Geophys. Res.* 97, 1097.
- Chum, J., Santolik, O., 2005. Propagation of whistler mode chorus to low altitudes: divergent ray trajectories and ground accessibility. *Ann. Geophys.* 23, 3727–3738.
- Church, S.R., Thorne, R.M., 1983. On the origin of plasmaspheric hiss: ray path integrated amplification. *J. Geophys. Res.* 88, 7941–7957.
- Cornilleau-Wehrin, N., Gendrin, R., Lefeuvre, F., Parrot, M., Grard, R., Jones, D., Bahnsen, A., Ungstrup, E., Gibbons, W., 1978. VLF electromagnetic waves observed onboard GEOS-1. *Space Sci. Rev.* 22, 371.
- Cornilleau-Wehrin, N., Solomon, J., Korth, A., Kremser, G., 1985. Experimental study of the relationship between energetic electrons and ELF waves observed on board GEOS: a support to quasilinear theory. *J. Geophys. Res.* 90, 4141.
- Dowden, R.L., 1971. Distinctions between mid latitude VLF hiss and discrete emissions. *Planet. Space Sci.* 19, 374.
- Dowden, R.L., Holzworth, R.H., 1990. Longitudinal variation of mid-latitude hiss from six long duration balloon flights. *J. Geophys. Res.* 95, 10,599.
- Draganov, A.B., Inan, U.S., Sonwalkar, V.S., Bell, T.F., 1992. Magnetospherically reflected whistlers as a source of plasmaspheric hiss. *Geophys. Res. Lett.* 19, 233.
- Draganov, A.B., Inan, U.S., Sonwalkar, V.S., Bell, T.F., 1993. Whistlers and plasmaspheric hiss: wave directions and three-dimensional propagation. *J. Geophys. Res.* 98, 11,401.
- Ellis, G.R.A., 1959. Low frequency electromagnetic radiation associated with magnetic disturbances. *Planet. Space Sci.* 1, 253.
- Etcheto, J., Gendrin, R., Solomon, J., Roux, A., 1973. A self-consistent theory of magnetospheric ELF hiss. *J. Geophys. Res.* 78, 8150.
- Fisher, R.K., Gould, R.W., 1969. Resonance cones in the field pattern of a short antenna in an anisotropic plasma. *Phys. Rev. Lett.* 22 (21), 1093–1095.
- Goldstein, B.E., Tsurutani, B.T., 1984. Wave normal directions of chorus near the equatorial source region. *J. Geophys. Res.* 89, 2789–2810.
- Goldstein, J., Sandel, B.R., Thomsen, M.F., Spasojevic, M., Reiff, P.H., 2004. Simultaneous remote sensing and in situ observations of plasmaspheric drainage plumes. *J. Geophys. Res.* 109, A03202.
- Green, J.L., Boardsen, S., Garcia, L., Taylor, W.W.L., Fung, S.F., Reinisch, B.W., 2005. On the origin of whistler mode radiation in the plasmasphere. *J. Geophys. Res.* 110, A03201.
- Green, J.L., et al., 2006. Reply to comment on “on the origin of whistler mode radiation in the plasmasphere” by Green et al. *J. Geophys. Res.* 111, A09211.
- Gross, S.H., Larocca, N., 1972. Phenomenological study of LHR hiss. *J. Geophys. Res.* 77, 1146.
- Gurnett, D.A., O'Brien, B.J., 1964. High-latitude geophysical studies with satellite Injun 3: 5. Very-low-frequency electromagnetic radiation. *J. Geophys. Res.* 69, 65–89.
- Harang, L., 1968. VLF-emissions observed at stations close to the auroral zone and at stations on lower latitude. *J. Atmos. Terr. Phys.* 30, 1143.
- Hattori, K., Hayakawa, M., Lagoutte, D., Parrot, M., Lefeuvre, F., 1991. Further evidence of triggering chorus emissions from wavelets in the hiss band. *Planet. Space Sci.* 39 (11), 1465–1472.
- Hayakawa, M., Tanaka, Y., Ohtsu, J., 1975. The morphologies of low latitude and auroral VLF “hiss”. *J. Atmos. Terr. Phys.* 37, 517.
- Hayakawa, M., Bullough, K., Kaiser, T.R., 1977. Properties of storm-time magnetospheric VLF emissions as deduced from the Ariel-3 satellite and ground-based observations. *Planet. Space Sci.* 25, 353.
- Hayakawa, M., Yamanaka, Y., Parrot, M., Lefeuvre, F., 1984. The wave normals of magnetospheric chorus emissions observed on board GEOS 2. *J. Geophys. Res.* 89, 2811–2821.
- Hayakawa, M., Parrot, M., Lefeuvre, F., 1986. The wave normals of ELF hiss emissions observed on board GEOS-1 at the equatorial and off equatorial regions of the plasmasphere. *J. Geophys. Res.* 91, 7989.
- Hayakawa, M., Sazhin, S.S., 1992. Mid-latitude and plasmaspheric hiss: a review. *Planet. Space Sci.* 40 (10), 1325–1338.
- Helliwell, R.A., Crystal, T.L., 1973. A feedback model of cyclotron interaction between whistler-mode and energetic electrons in the magnetosphere. *J. Geophys. Res.* 78, 7357.
- Helliwell, R.A., Inan, U.S., 1982. VLF wave growth and discrete emission triggering in the magnetosphere: a feedback model. *J. Geophys. Res.* 87, 3537.
- Helliwell, R.A., 1989. Resonance interaction between energetic electrons and whistler mode waves at the Gendrin angle. *Eos. Trans., AGU* 70, 440.
- Horne, R.B., Thorne, R.M., Meredith, N.P., Anderson, R.R., 2003. Diffuse auroral electron scattering by electron cyclotron harmonic and whistler mode waves during an isolated substorm. *J. Geophys. Res.* 108 (A7), 1290.
- Huang, C.Y., Goertz, C.K., 1983. Ray-tracing studies and path-integrated gains of ELF unducted whistler-mode waves in the Earth's magnetosphere. *J. Geophys. Res.* 88, 7927.
- Huang, C.Y., Goertz, C.K., Anderson, R.R., 1983. A theoretical study of plasmaspheric hiss generation. *J. Geophys. Res.* 88, 7927–7940.
- Inan, U.S., Platino, M., Bell, T.F., Gurnett, D.A., Pickett, J.S., 2004. Cluster measurements of rapidly moving sources of ELF/VLF chorus. *J. Geophys. Res.* 109 (A5), A05214.
- Jorgensen, T.S., 1966. Morphology of VLF hiss zones and their correlation with particle precipitation events. *J. Geophys. Res.* 71, 1367.
- Katoh, Y., Omura, Y., 2007. Computer simulation of chorus wave generation in the Earth's inner magnetosphere. *Geophys. Res. Lett.* 34, L03102.

- Kelley, M.C., Tsurutani, B.T., Moser, F.S., 1975. Properties of ELF electromagnetic waves in and above the Earth's ionosphere deduced from plasma wave experiment on OVI-17 and OGO-6 satellites. *J. Geophys. Res.* 80, 4603.
- Kelley, M.C., Heelis, R.A., 1989. *The Earth's Ionosphere: Plasma Physics and Electrodynamics*. Academic Press, New York.
- Koons, H.C., 1981. The role of hiss in magnetospheric chorus emissions. *J. Geophys. Res.* 86, 6745–6754.
- Kovner, M.S., Kuznetsova, V.A., Likhter, Ya.L., 1978. Ionospheric generation of ELF emissions. *Geomagn. Aeron. (English translation)* 18, 313.
- Lam, M.M., Horne, R.B., Meredith, N.P., Glauert, S.A., 2007. Modeling the effects of radial diffusion and plasmaspheric hiss on outer radiation belt electrons. *Geophys. Res. Lett.* 34, L20112.
- LeDocq, M.J., Gurnett, D.A., Hospodarsky, G.B., 1998. Chorus source locations from VLF Poynting flux measurements with the Polar spacecraft. *Geophys. Res. Lett.* 25, 4063–4066.
- Lauben, D.S., Inan, U.S., Bell, T.F., 2002. Source characteristics of ELF/VLF chorus. *J. Geophys. Res.* 107, 1429.
- Lyons, L.R., Thorne, R.M., Kennel, C.F., 1972. Pitch-angle diffusion of radiation belt electrons within the plasmasphere. *J. Geophys. Res.* 77, 3455–3474.
- Lyons, L.R., Thorne, R.M., 1973. Equilibrium structure of radiation belt electrons. *J. Geophys. Res.* 78 (13), 2142–2149.
- Meredith, N.P., Horne, R.B., Anderson, R.R., 2001. Substorm dependence of chorus amplitudes: Implications for the acceleration of electrons to relativistic energies. *J. Geophys. Res.* 106 (A6), 13,165.
- Meredith, N.P., Horne, R.B., Thorne, R.M., Anderson, R.R., 2003. Favored regions for chorus-driven electron acceleration to relativistic energies in the Earth's outer radiation belt. *Geophys. Res. Lett.* 30 (16), 1871.
- Meredith, N.P., Horne, R.B., Thorne, R.M., Summers, D., Anderson, R.R., 2004. Substorm dependence of plasmaspheric hiss. *J. Geophys. Res.* 109, A06209.
- Meredith, N.P., Horne, R.B., Glauert, S.A., Thorne, R.M., Summers, D., Albert, J.M., Anderson, R.R., 2006a. Energetic outer zone electron loss timescales during low geomagnetic activity. *J. Geophys. Res.* 111, A05212.
- Meredith, N.P., Horne, R.B., Clilverd, M.A., Horsfall, D., Thorne, R.M., Anderson, R.R., 2006b. Origins of plasmaspheric hiss. *J. Geophys. Res.* 111, A09217.
- Meredith, N.P., Horne, R.B., Glauert, S.A., Anderson, R.R., 2007. Slot region electron loss timescales due to plasmaspheric hiss and lightning generated whistlers. *J. Geophys. Res.* 112, A08214.
- Meredith, N.P., Horne, R.B., Anderson, R.R., 2008. Survey of magnetosonic waves and proton ring distributions in the Earth's inner magnetosphere. *J. Geophys. Res.* 113 (A6), A06213.
- Molchanov, O.A., Parrot, M., Mogilevski, M.M., Lefeuve, F., 1991. A theory of PLHR emissions to explain the weekly variation of ELF data observed by a low-latitude satellite. *Ann. Geophys.* 9 (10), 669–680.
- Muto, H., Hayakawa, M., 1987. Ray-tracing study of the propagation in the magnetosphere of whistler-mode VLF emissions with frequency above one half the gyrofrequency. *Planet. Space Sci.* 35 (11), 1397–1404.
- Muzzio, J.L.R., Angerami, J.J., 1972. OGO-4 Observations of extremely low frequency hiss. *J. Geophys. Res.* 77, 1157.
- Ni, B., Thorne, R.M., Shprits, Y.Y., Bortnik, J., 2008. Resonant scattering of plasma sheet electrons by whistler-mode chorus: Contribution to diffuse auroral precipitation. *Geophys. Res. Lett.* 35, L11106.
- Nunn, D., Sazhin, S.S., 1991. On the generation mechanism of hiss-triggered chorus. *Ann. Geophys.* 9, 603–613.
- Omura, Y., Nunn, D., Matsumoto, H., Rycroft, M.J., 1991. A review of observational, theoretical and numerical studies of VLF triggered emissions. *J. Atmos. Terr. Phys.* 53, 351–358.
- Omura, Y., Katoh, Y., Summers, D., 2008. Theory and simulation of the generation of whistler-mode chorus. *J. Geophys. Res.* 113, A04223.
- Ondoh, T., Nakamura, Y., Watanabe, S., Aikyo, K., Murakami, T., 1980. Narrow-band VLF hiss observed in the vicinity of the plasmapause. *J. Radio Res. Lab.* 27, 131.
- Ondoh, T., Nakamura, Y., Watanabe, S., Murakami, T., 1981. Narrow-band 5 kHz hiss observed in the vicinity of the plasmapause. *Planet. Space Sci.* 29, 65.
- Ondoh, T., Nakamura, Y., Watanabe, S., Aikyo, K., Murakami, T., 1982. Plasmaspheric ELF hiss observed by ISIS satellites. *J. Radio Res. Labs.* 29, 159.
- Ondoh, T., Nakamura, Y., Watanabe, S., Aikyo, K., Murakami, T., 1983. Plasmaspheric hiss observed in the topside ionosphere at mid- and low-latitudes. *Planet. Space Sci.* 31, 411.
- Parady, B.K., 1974. Anisotropic proton instability for magnetospheric (APIM) hiss: an introduction. *Geophys. Res. Lett.* 1, 235.
- Parady, B.K., Eberlein, D.D., Marvin, J.A., Taylor, W.W.L., Cahill Jr., L.J., 1975. Plasmaspheric hiss observations in the evening and afternoon quadrants. *J. Geophys. Res.* 80, 2183.
- Parrot, M., Lefeuve, F., 1986. Statistical study of the propagation characteristics of ELF hiss observed on GEOS 1, inside and outside the plasmapause. *Ann. Geophys.* 4, 363.
- Parrot, M., Molchanov, O.A., Mogilevski, M.M., Lefeuve, F., 1991. Daily variations of ELF data observed by a low-altitude satellite. *Geophys. Res. Lett.* 18, 1039.
- Parrot, M., Santolik, O., Cornilleau-Wehrin, N., Maksimovich, M., Harvey, C., 2003. Magnetically reflected chorus waves revealed by ray tracing with CLUSTER data. *Ann. Geophys.* 21 (5), 1111–1120.
- Parrot, M., Santolik, O., Gurnett, D., Pickett, J., Cornilleau-Wehrin, N., 2004. Characteristics of magnetospherically reflected chorus waves observed by Cluster. *Ann. Geophys.* 22, 2597–2606.
- Rao, M., Somayajulu, V.V., Tantry, B.A.P., 1972. An analysis of multi-station ground observations of VLF hiss. *J. Geomagn. Geoelectr.* 24, 261.
- Rodger, C.J., Clilverd, M.A., 2008. Hiss from chorus. *Nature* 452, 41.
- Russell, C.T., Holzer, R.E., Smith, E.J., 1969. OGO 3 observations of ELF noise in the magnetosphere: 1. Spatial extent and frequency of occurrence. *J. Geophys. Res.* 74, 755–777.
- Santolik, O., Parrot, M., 1999. Case studies on wave propagation and polarization of ELF emissions observed by Freja around the local proton gyrofrequency. *J. Geophys. Res.* 104, 2459–2475.
- Santolik, O., Parrot, M., Storey, L.R.O., Pickett, J.S., Gurnett, D.A., 2001. Propagation analysis of plasmaspheric hiss using Polar PWI measurements. *Geophys. Res. Lett.* 28 (6), 1127–1130.
- Santolik, O., Gurnett, D.A., Pickett, J.S., Parrot, M., Cornilleau-Wehrin, N., 2003. Spatio-temporal structure of storm-time chorus. *J. Geophys. Res.* 108 (A7), 1278.
- Santolik, O., Gurnett, D.A., 2003. Transverse dimensions of chorus in the source region. *Geophys. Res. Lett.* 30 (2), 1031.
- Santolik, O., Gurnett, D.A., Pickett, J.S., 2004. Multipoint investigation of the source region of storm-time chorus. *Ann. Geophys.* 22, 2555–2563.
- Santolik, O., Chum, J., Parrot, M., Gurnett, D.A., Pickett, J.S., Cornilleau-Wehrin, N., 2006. Propagation of whistler mode chorus to low altitudes: Spacecraft observations of structured ELF hiss. *J. Geophys. Res.* 111, A10208.
- Sazhin, S.S., 1984. A model for hiss-type mid-latitude VLF emissions. *Planet. Space Sci.* 32, 1263.
- Sazhin, S.S., 1989. Improved quasilinear models of parallel whistler-mode instability. *Planet. Space Sci.* 37, 633.
- Smith, E.J., Frandsen, A.M.A., Tsurutani, B.T., Thorne, R.M., Chan, K.W., 1974. Plasmaspheric hiss intensity variations during magnetic storms. *J. Geophys. Res.* 79 (16), 2507–2510.
- Solomon, J., Cornilleau-Wehrin, N., Korth, A., Kremser, G., 1988. An experimental study of ELF/VLF hiss generation in the Earth's magnetosphere. *J. Geophys. Res.* 93, 1839–1847.
- Sonwalkar, V.S., Inan, U.S., 1989. Lightning as an embryonic source of VLF hiss. *J. Geophys. Res.* 94, 6986.
- Stenzel, R.L., 1976. Antenna radiation patterns in the whistler wave regime measured in a large laboratory plasma. *Radio Science* 11, 1045–1056.
- Storey, L.R.O., Lefeuve, F., 1979. The analysis of 6-component measurements of a random electromagnetic wave field in a magnetoplasma, 1. The direct problem. *Geophys. J. R. Astron. Soc.* 56, 255–270.
- Storey, L.R.O., Lefeuve, F., Parrot, M., Cairo, L., Anderson, R., 1991. Initial survey of the wave distribution functions for plasmaspheric hiss observed by ISEE 1. *J. Geophys. Res.* 96, 19469–19489.
- Summers, D., Ni, B., Meredith, N.P., 2007. Timescales for radiation belt electron acceleration and loss due to resonant wave particle interactions: 2. Evaluation for VLF chorus, ELF hiss, and EMIC waves. *J. Geophys. Res.* 112, A04207.
- Summers, D., Ni, B., Meredith, N.P., Horne, R.B., Thorne, R.M., Moldwin, M.B., Anderson, R.R., 2008. Electron scattering by whistler-mode (ELF) hiss in plasmaspheric plumes. *J. Geophys. Res.* 113, A04219.
- Thorne, R.M., Smith, E.J., Burton, R.K., Holzer, R.E., 1973. Plasmaspheric hiss. *J. Geophys. Res.* 78, 1581–1595.
- Thorne, R.M., Church, S.R., Malloy, W.J., Tsurutani, B.T., 1977. The local time variation of ELF emissions during periods of substorm activity. *J. Geophys. Res.* 82, 1585.
- Thorne, R.M., Church, S.R., Gorney, D.J., 1979. On the origin of plasmaspheric hiss: the importance of wave propagation and the plasmapause. *J. Geophys. Res.* 84, 5241.
- Thorne, R.M., Horne, R.B., Meredith, N.P., 2006. Comment on On the origin of whistler mode radiation in the plasmasphere by Green et al. *J. Geophys. Res.* 111, A09210.
- Trakhtengerts, V.Y., 1999. A generation mechanism for chorus emissions. *Ann. Geophys.* 17, 95–100.
- Tsurutani, B.T., Smith, E.J., Thorne, R.M., 1975. Electromagnetic hiss and relativistic electron losses in the inner zone. *J. Geophys. Res.* 80 (4), 600–607.
- Wang, T.N.C., Bell, T.F., 1969. Radiation resistance of a short dipole immersed in a cold magnetoionic medium. *Radio Sci.* 4 (2), 167–177.
- Wang, T.N.C., Bell, T.F., 1972. VLF/ELF input impedance of an arbitrarily oriented loop antenna in a cold, collisionless multicomponent magnetoplasma. *IEEE Trans. Antennas Propagation (Commun.)* AP-20, 394–398.
- Wang, T.N.C., Bell, T.F., 1973. On input impedance of an arbitrarily oriented small loop antenna in a cold collisionless magnetoplasma. *IEEE Trans. Antennas Propagation (Commun.)* 21 (5), 745–746.
- Wang, H.K., Goldstein, M.L., 1988. Proton beam generation of oblique whistler-mode waves. *J. Geophys. Res.* 93, 4110.